Received: 23 October 2021

DOI: 10.1002/mop.33186

WILEY

RESEARCH ARTICLE

Numerical simulation and analysis of dual base transistor laser

Ramakrishnan Ranjith[1] | **Shanmugasundaram Piramasubramanian**[2] | **Muthu Ganesh Madhan**[2]

[1]Department of Electronics and Communication Engineering, Government College of Engineering Bargur, Bargur, India

[2]Department of Electronics Engineering, Madras Institute of Technology Campus, Anna University Chennai, Chennai, India

Correspondence
Ramakrishnan Ranjith, Department of Electronics and Communication Engineering, Government College of Engineering Bargur, Bargur, Tamil Nadu, India.
Email: rranjithmtm@gmail.com

Abstract

In this work, characteristics of dual base transistor laser are numerically analyzed for the first time. Active base region of the transistor laser is split into two unequal regions composing of shorter and longer sections, which are biased separately. Static characteristics of transistor laser are evaluated using a rate equation model, which reveals switching action in output optical power for a longer section base current of 9.2 mA with unpumped shorter section. Hysteresis behavior in the optical output is observed for the longer section input current till 1.6 mA. Optical bistable characteristics are studied for various values of gain (longer) and absorber (shorter) section currents. Further slope efficiency is evaluated using P-I characteristics, before the onset of bistability, for gain lever features under common emitter (CE) configuration. A maximum gain lever of 4.5 dB is observed with the longer section bias current of 1.3 mA.

KEYWORDS

bistability effect in transistor laser, dual base transistor laser, modeling of transistor laser, numerical analysis of transistor laser

[Correction added on February 21, 2022, after first online publication: Authors first and last names was updated.]

1 | INTRODUCTION

Large optical gain in laser diodes finds numerous applications in digital optical logic circuits, high speed switching and for obtaining high modulation depth in direct modulation.[1–10] Gain switching provides higher optical power output for the given electrical input in active optical devices and is useful to overcome the coupling and transmission losses in the passive waveguides. Gain lever laser diodes have interesting property of providing maximum gain for a particular current compared to normal laser diode. Gain lever laser diodes are investigated for radio over fiber applications and digital switching.[6–12] Gain lever effect in laser diodes is realized by splitting the active region into two isolated sections with ratio ranging from 0.1 to 0.9. Due to sub linear nature of the gain versus carrier density characteristics in quantum well active regions, a large change in the carrier density in one section of the laser (longer section) results due to a small change in injection current in the other section (shorter section). Both sections have different value of differential gain.[1–5] Currently, the switching speed of the electronic circuits in computer/processors is limited by RC time constant and carrier transit time. To overcome the problem, opto-electronics based logic circuits are considered as a potential replacement.[13] Bistability occurs in electrical or optical systems in which there is a region for which the output has two stable energy states for a given input. Switching between these values can be achieved by a change in the input level. Hence, bistable optical active devices find applications in optical switching and digital optical integrated circuits.

Bistability in laser diodes was first observed by Lasher et al.[1] and the proposed device had two sections of active region, one light emitting region and another absorbing region, with unequal lengths. Ueno et al.[2] assumed two sections of active regions with different value of differential gain, carrier lifetime and analyzed the bistable operation in laser diodes. Circuit modeling of bistability in twin section laser diodes and the effect of load and source resistance were reported.[3–6] Thermal effects in bistable laser were also investigated.[4,5] Vahala et al.[3] observed a novel gain lever mechanism with 6 dB improvement in electrical and optical modulation response of quantum well laser diode. The sections in active region were considered as master and slave regions with later having higher modal gain compared to the former. Moore et al.[4] reported 40 dB enhancement in the efficiency of transmission of microwave signals by single quantum well laser diode with two sections. Frequency dependency of the gain lever phenomenon is reported with enhancement factor dropping to 15 dB, at the relaxation

oscillation frequencies. Lau et al.[4] observed that gain lever effect in two section laser diode enhances the Frequency Modulation (FM) performance of the laser without enhancing the FM noise. Duan et al.[5] proposed a theoretical model for the bistable laser diode by introducing the dependence law of transition time and turn-on-jitter on injection currents. It is found that, for a constant current input in active section, the rise time decreases and fall time increases with injection current in the other section. Wang et al.[7] analyzed the dynamic characteristics of bistable laser diode with parameters that influence turn-on and turn-off dynamics. Pocha et al.[8] evaluated the electrical and optical gain lever effect in double quantum well InGaAs laser diode and reported an AM efficiency enhancement of 7 and 4 dB in electrical and optical gain respectively, compared to normal laser diode. Piramasubramanian et al.[9] analyzed the modulation performance of gain levered laser diode in the fiber optic link. A 12 dB enhancement in extinction ratio (ER) is reported for gain levered laser diode compared with normal laser diode.

Transistor laser (TL) is a three terminal device consisting of emitter, base and collector regions with quantum well at the base region. It can be modeled as a three port device with two electrical ports and one optical port. Carriers from the emitter region are captured by the quantum well in the base region before they are collected by the reverse biased collector region.[14–17] Current gain in the TL is limited by the radiative recombination process in the quantum well region. The carriers escaping the quantum well are collected by the reverse biased collector region.[14–17] TL is characterized by lower carrier lifetime compared to the diode laser, due to the applied reverse bias potential in collector–base junction. Moreover, TL offers higher bandwidth than diode laser and finds application potential in high speed optical communication. The first TL at emission wavelength of 980 nm was fabricated by the Feng et al. and demonstrated at room temperature along with charge control analysis.[14–16] A number of mathematical models have been proposed based on the operation of TL. The most popular scheme termed as "triangular charge control model" was proposed by Zhang et al.,[18] by considering the charge in the base region as triangular profile. They determined base charge density, quantum well carrier density and photon density.[18] The effects of carrier capture and carrier escape time were considered by Faraji et al. They also proposed the common base and common emitter modeling of TL with terminal current densities.[19] Harmonic analysis of an output of a TL with mixed signal as an input is analyzed by Feng et al.[15] Large signal analysis has been carried out for 1300 nm TL and its performance has been compared with laser diode.[20] The device was fabricated in NPN and PNP configurations with six quantum wells and demonstrated at room temperature by Shirao et al.[17] Harmonic analysis of TL with different number of quantum wells in the base region achieving lower distortion under common base configuration is reported[21,22] and further the distortion reduction mechanisms are also discussed.[23]

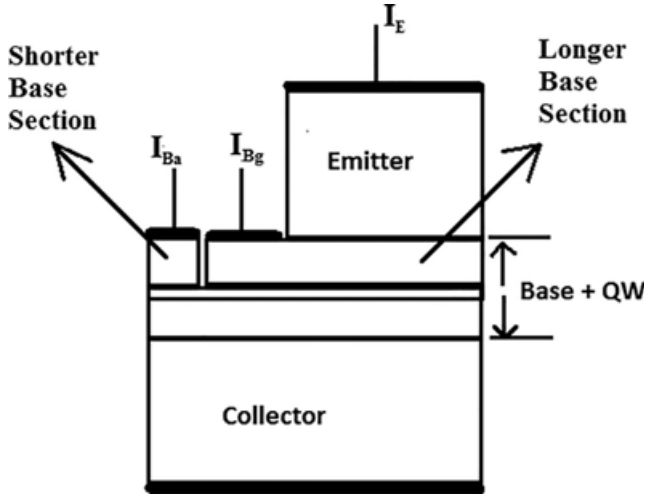

FIGURE 1 Proposed structure of dual base transistor laser (TL)

In this work, gain lever and bistable effects are analyzed in TL under common emitter configuration, for the first time. The active region in the base of the TL is split into two sections to exhibit gain lever effect. The rate equations which model the TL incorporating dual base regions are numerically solved by fourth order Runge–Kutta method. Static characteristics and gain lever are evaluated in CE configuration. A maximum of 4.5 dB increase in gain is observed for the two sectioned TL.

2 | RATE EQUATION MODEL OF DUAL BASE TL

The active region of TL is split into two sections, longer (g) and shorter unit (a). Both regions are biased with different currents, leading to unequal gains. The modal gain of longer section (G_g) is assumed to be greater than the shorter one (G_a). Due to highly sublinear nature of gain versus carrier density characteristics in quantum well, a large carrier density variation in longer section is obtained for a small change in the applied current to the shorter section of a dual base TL. This effect is expected to enhance the modulation efficiency of the TL. The current input applied to the longer and shorter base sections are denoted as I_{bg} and I_{ba} respectively, as shown in Figure 1. Sections "a" and "b" are also referred to as control and slave regions.

The rate equation model of TL is formed by considering the boundary conditions and solving the second order differential electron diffusion equation in the base region of the TL. A triangular profile of the charge distribution in the base region satisfies the boundary conditions as shown in the Figure 2. A virtual state is considered above the two-dimensional quantum well to denote the carrier concentration at that point (N_{vs}).

An NPN heterostructure based TL is considered for this analysis and the band structure at the base region of the TL is

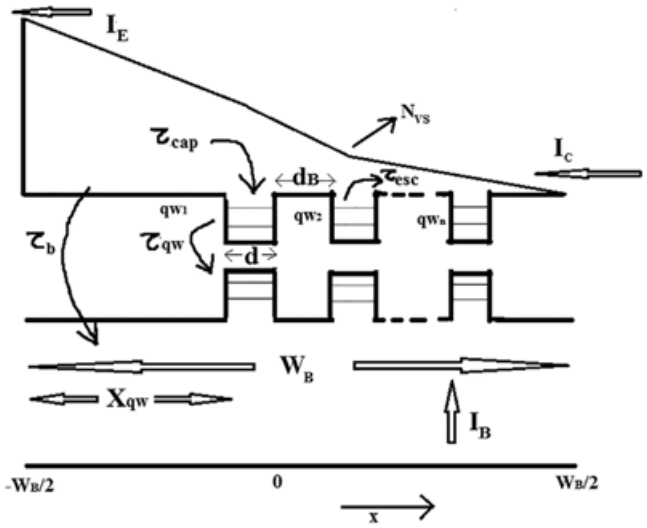

FIGURE 2 Triangular charge model in base region of transistor laser (TL)[19]

depicted in Figure 2. W_b denotes the width of the base region and d denotes the quantum well width. Current direction in the above figure is based on the conventional current flow.

$$\frac{\partial \delta n}{\partial t} = D_n \frac{\partial^2 \delta n}{\partial x^2} - \frac{\delta n}{\tau_B} \tag{1}$$

δn is the excess carrier concentration in the base region. The diffusion Equation (1) is considered for both longer and shorter section base regions and solved for the injected carriers from emitter under triangular charge profile as shown in Figure 2. Emitter current densities of longer and shorter section regions are found by using the equations given below.

$$J_{Eg} = qD_n \frac{\partial \delta n_g}{\partial x} \text{ at } x = -\frac{W_B}{2} \tag{2}$$

$$J_{Ea} = qD_n \frac{\partial \delta n_a}{\partial x} \text{ at } x = -\frac{W_B}{2} \tag{3}$$

δn_g and δn_a are the excess carriers concentration present in longer section and shorter section of the active region. The TL is assumed to be biased at active region with reverse bias potential at collector–base junction. Hence the following boundary conditions are assumed as below.

$$\frac{\partial \delta n_g}{\partial x} = \frac{\partial \delta n_a}{\partial x} = 0 \text{ at } x = \frac{W_B}{2} \tag{4}$$

Based on the triangular charge model and boundary conditions, the virtual state electron density in the longer (N_{vsg}) and shorter section (N_{vsa}) of the base region are obtained by solving the Equation (1).

The laser rate equations for the dual base TL describing the virtual state carrier density in longer and shorter sections, quantum well carrier density in longer and shorter sections and photo density are

$$\frac{dN_{vsg}}{dt} = -\frac{N_{vsg}}{\tau_{cap}} - \frac{N_{QWg}}{\tau_{esc}} + \frac{I_{vsg}}{l_g dqa} \tag{5}$$

$$\frac{dN_{vsa}}{dt} = -\frac{N_{vsa}}{\tau_{cap}} - \frac{N_{QWa}}{\tau_{esc}} + \frac{I_{vsa}}{l_a dqa} \tag{6}$$

Virtual state is defined as the unconfined state just above the confined quantum states. N_{QWg} and N_{QWa} are the quantum well carrier densities present in the longer and shorter sections of the TL base. Current entering into the longer and shorter section of the quantum well are denoted as I_{vsg} and I_{vsa} respectively. τ_{cap} and τ_{esc} denotes carrier capture and escape time between the virtual state and the quantum well.

$$\frac{dN_{QWg}}{dt} = \frac{N_{vsg}}{\tau_{cap}} - \frac{N_{QWg}}{\tau_{esc}} - \frac{G'_g S\left(N_{QWg} - N_g\right)}{1 + \epsilon_{other} S} - \frac{N_{QWg}}{\tau_s} \tag{7}$$

$$\frac{dN_{QWa}}{dt} = \frac{N_{vsa}}{\tau_{cap}} - \frac{N_{QWa}}{\tau_{esc}} - \frac{G'_a S\left(N_{QWa} - N_g\right)}{1 + \epsilon_{other} S} - \frac{N_{QWa}}{\tau_s} \tag{8}$$

Equations (7) and (8) represent the quantum well electron density in the longer (N_{QWg}) and shorter (N_{QWa}) sections respectively. G'_g and G'_a defines the differential gain in the longer and shorter sections of the active region respectively. ϵ_{other} is the nonlinear gain compression factor due to spectral hole burning and carrier heating effect. N_g is the transparency carrier density, which is used to achieve the population inversion in quantum well for stimulated emission and τ_s is quantum well electron life time.

$$\frac{dS}{dt} = \frac{l_g \epsilon G'_g S\left(N_{QWg} - N_g\right)}{1 + \epsilon_{other} S} + \frac{l_a \epsilon G'_a S\left(N_{QWa} - N_g\right)}{1 + \epsilon_{other} S} - \frac{S}{\tau_p} + l_g C \frac{N_{QWg}}{\tau_s} + l_a C \frac{N_{QWa}}{\tau_s} \tag{9}$$

Equation (9) gives rate of change of photon density in the quantum well, τ_p is the photon life time in the active region and C is the spontaneous recombination coefficient. Solving the above coupled rate Equations (5)–(9), provides the photon density, electron density present in the virtual state and quantum well in both longer and shorter sections of the active region.

$$J_{Eg} = N_{vsg} \frac{qD_n}{L_D} \left(\sinh\left(\frac{W_b}{L_D}\right) + \frac{\cosh^2\left(\frac{W_b}{L_D}\right)}{\sinh\left(\frac{W_B}{L_D}\right)} \right) + J_{VSg} \cosh\left(\frac{W_b}{2L_D}\right) \tag{10}$$

$$J_{Ea} = N_{vsa} \frac{qD_n}{L_D} \left(\sinh\left(\frac{W_b}{L_D}\right) + \frac{\cosh^2\left(\frac{W_b}{L_D}\right)}{\sinh\left(\frac{W_B}{L_D}\right)} \right) + J_{VSa} \cosh\left(\frac{W_b}{2L_D}\right) \tag{11}$$

$$J_E = J_{Eg} + J_{Ea} \tag{12}$$

By solving Equations (2) and (3), emitter current densities entering in longer and shorter sections are evaluated and

represented in Equations (10) and (11), where W_b and L_D defines the base width and diffusion length of the charge carrier in the base region. J_{VSa} is the virtual state current density entering the quantum well from the virtual state in the base region. Equation (13) and (14) give the expressions for base current density due to radiative and non-radiative recombination of carriers in both shorter and longer sections of the active region.

$$J_{Ba} = 2N_{vas}\frac{qD_n}{L_D}\sinh\left(\frac{W_b}{L_D}\right) + J_{VSa}\cosh\left(\frac{W_b}{2L_D}\right) \quad (13)$$

$$J_{Bg} = 2N_{vag}\frac{qD_n}{L_D}\sinh\left(\frac{W_b}{L_D}\right) + J_{VSg}\cosh\left(\frac{W_b}{2L_D}\right) \quad (14)$$

The collector current density arising due to carriers removed by the collector region from both longer and shorter sections of base region is given by Equation (15).

$$J_C = N_{vsa}\frac{qD_n}{L_D}\left(\frac{\cosh^2\left(\frac{W_b}{L_D}\right)}{\sinh\left(\frac{W_b}{L_D}\right)}\right) + N_{vsag}\frac{qD_n}{L_D}\left(\frac{\cosh^2\left(\frac{W_b}{L_D}\right)}{\sinh\left(\frac{W_b}{L_D}\right)}\right) \quad (15)$$

The optical gain present in the longer and shorter sections are defined as

$$G_g = g_0\ln\left(\frac{N_{QWg}+N_S}{N_t+N_S}\right) \quad (16)$$

TABLE 1 Dual base TL parameters[20]

Parameter	Value	Symbols
Well thickness	5 nm/well	d
Longer section length fraction	0.9	l_g
Shorter section length fraction	0.1	l_a
Barrier length	10 nm	d_B
Stripe width	2 μm	W
Cavity length	250 μm	L
Total base width	250 nm	W_b
Reflectivity	0.3, 0.9	R
Material gain for longer section	3600/cm	g_{og}
Material gain for shorter section	3600/cm	g_{oa}
Optical confinement factor	0.011/well	ϵ
Internal loss	5/cm	α_i
Gain compression factor	$0.5 \times 10^{-17}/cm^3$	ϵ_{other}
Recombination coefficient	$1.55 \times 10^{-10}/cm^3s$	B_{eff}
Spontaneous emission coefficient	10^{-6}	C
Carrier lifetime in base	1 ns	τ_s
Capture time	1 ps	τ_{cap}
Escape time	1 ns	τ_{esc}
Photon life time	4.1 ps	τ_p

Abbreviation: TL, transistor laser.

$$G_a = g_0\ln\left(\frac{N_{QWa}+N_S}{N_t+N_S}\right) \quad (17)$$

A logarithmic relation between carrier density and gain of the quantum well is considered, where g_0 is the material gain, N_t is transparency carrier density and N_S is the fitting parameter.

The diffusion length (L_D) is expressed as

$$L_D = \sqrt{\frac{D_n\tau_b}{1+j\omega\tau_b}} \quad (18)$$

where ω and τ_b define angular frequency and base recombination lifetime. For $\omega = 0$, the diffusion length (D_n) is defined as

$$L_D = \sqrt{D_n\tau_b} \quad (19)$$

The rate Equations (5)–(9) of a dual base TL are solved numerically by 4th order Runge–Kutta method. The parameters used the above equations are given below (Table 1).

3 | SIMULATION RESULTS

3.1 | DC characteristics

A three quantum well, dual base TL is considered for this analysis. A constant current is given as an input to the rate equation model of the TL configured in common emitter configuration. Diffusion constant of the TL is denoted by $L_D = \sqrt{D_n\tau_b}$, the angular frequency is assumed to be $\omega = 0$ for DC analysis. By providing different input currents to both longer and shorter sections, the threshold current and optical powers are determined. The optical power emitted from the TL is calculated by the expression given below[11–13]

$$P = \eta v_g(\alpha_i+\alpha_m)hfS\frac{V}{2\epsilon} \quad (20)$$

where η is the external quantum efficiency, v_g is the group velocity and α_i and α_m are internal and mirror losses.

To validate our model, initially we consider a normal (shorted dual base) 3QW TL and solved the equations with an input current applied to the emitter terminal and plotted in Figure 3A. The P-I characteristics observed in Figure 3A matches with the characteristics of the 3QWTL in the literature.[20] TL under CE configuration is realized by forward biasing the base–emitter junction and reverse biasing the emitter–collector junction. An input current is applied to the base terminal of the dual base TL as shown in Figure 1. Optical power is evaluated for a range of input base currents and plotted in Figure 3B.

From Figure 3 it is found that the optical power increases after threshold current due to stimulated recombination. Prior to that, spontaneous recombination is significant. We repeat the simulation under dual base condition, where the

active region of the TL is divided into two sections, that is, longer (L_g) and shorter (L_a) with shorter to total length ratio (L_a/L) of 10%. Optical slope of the TL is analyzed by varying the longer and shorter section base current of the device separately, by maintaining the other current as constant as shown in the Figures 4 and 5.

From Figure 4 it is found that the optical power switches to a large value at threshold, unlike a normal TL (both

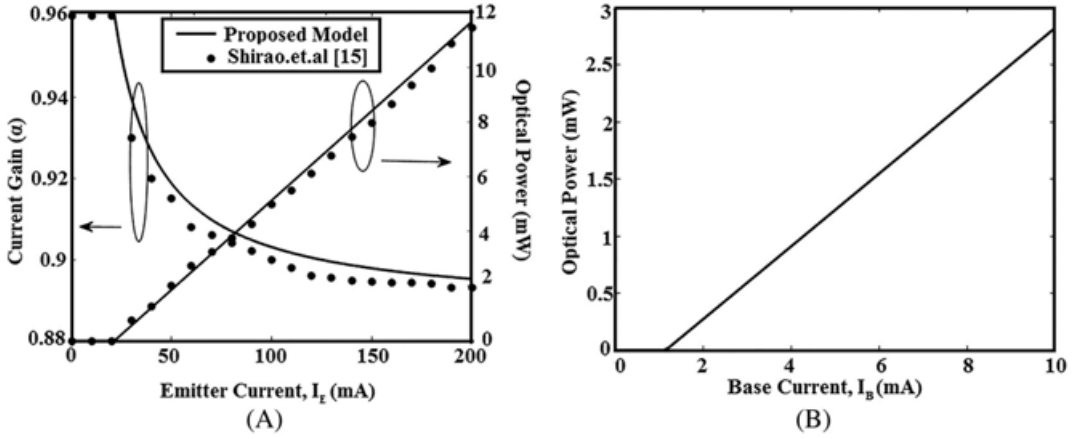

FIGURE 3 DC characteristics of single base 3QW transistor laser (TL) under: (A) CB configuration[20] and (B) CE configuration

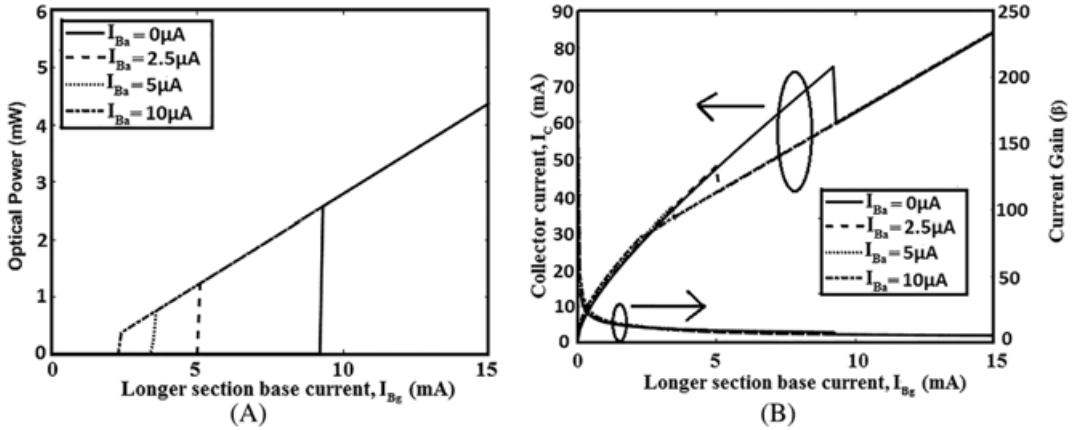

FIGURE 4 DC characteristics of dual base transistor laser (TL) with longer section bias currents (I_{Bg}): (A) optical power and (B) collector current and current gain

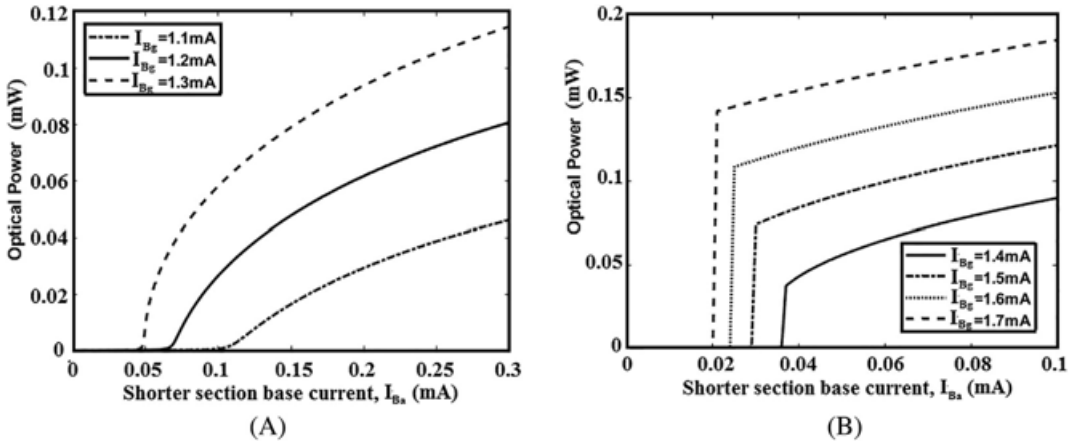

FIGURE 5 DC characteristics of gain lever transistor laser (TL) with constant longer section bias currents (I_{Eg}): (A) low bias currents and (B) high bias currents

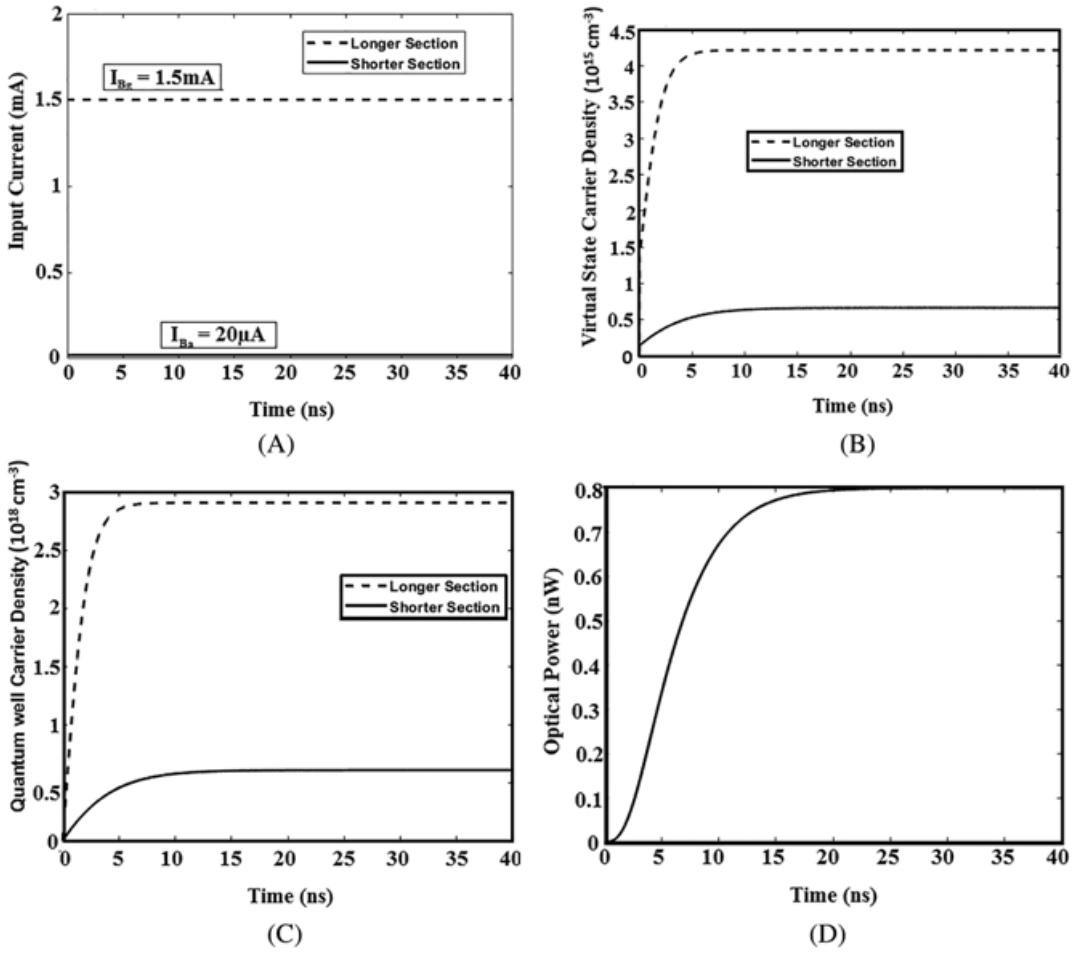

FIGURE 6 Transient analysis of dual base transistor laser (TL) before threshold: (A) input currents, (B) virtual state carrier density, (C) quantum well carrier density, and (D) optical power

sections shorted case) and increases further for increase in longer section currents (I_{Bg}) with fixed shorter section bias currents (I_{Ba}). For shorter section current of 0 mA, a switching in optical power of 2.53 mW is observed at 9.3 mA and it is found that the magnitude of switching power reduces for increasing the shorter section current. Further, the threshold current decreases for increasing shorter section bias currents (I_{Ba}) along with switching characteristics. Current gain (β) of dual base TL under CE configuration decreases as optical power increases for increasing the longer section current (I_{Bg}). Moreover, the collector current decreases sharply at the threshold current due to stimulated recombination and subsequent reduction in carrier density, as shown in the Figure 4. Under fixed longer section bias current, a small variation of shorter section base current in TL provides a large change in output power due to gain levering effect.

From the above Figure 5A,B it is found that, at constant values of longer section bias current (I_{Bg}) and varying the shorter section current (I_{Ba}) provides higher slope until 1.3 mA creating the gain lever effect. From Figure 5A the slope of the optical power is found to be decreasing for increase in the shorter section current (I_{Ba}). Conditions pertaining to larger slope can be used for gain levering. Moreover, it is observed that beyond longer section current of 1.3 mA, optical switching takes place due to the presence of absorber section in the cavity. The switching behavior occurs at lower values of absorber section current, when the gain section is biased heavily. It can be inferred from Figure 5B, for longer section current of 1.4 mA and beyond, varying the shorter section results in increase in the optical power and decrease in threshold.

3.2 | Transient analysis

The transient (time) characteristics of dual base TL with three quantum wells in the base region is analyzed by applying a DC input current of $I_{Bg} = 1.5$ mA, $I_{Ba} = 20$ μA (before threshold) and $I_{Ba} = 40$ μA (after threshold) as shown in Figures 6 and 7. Virtual state carrier density (N_{VS}), Quantum well carrier density (N_{QW}) and Optical power, for both longer and shorter sections for different input current are plotted in Figures 6 and 7. From Figures 6 and 7, it is observed that the relaxation oscillations occur after reaching the threshold

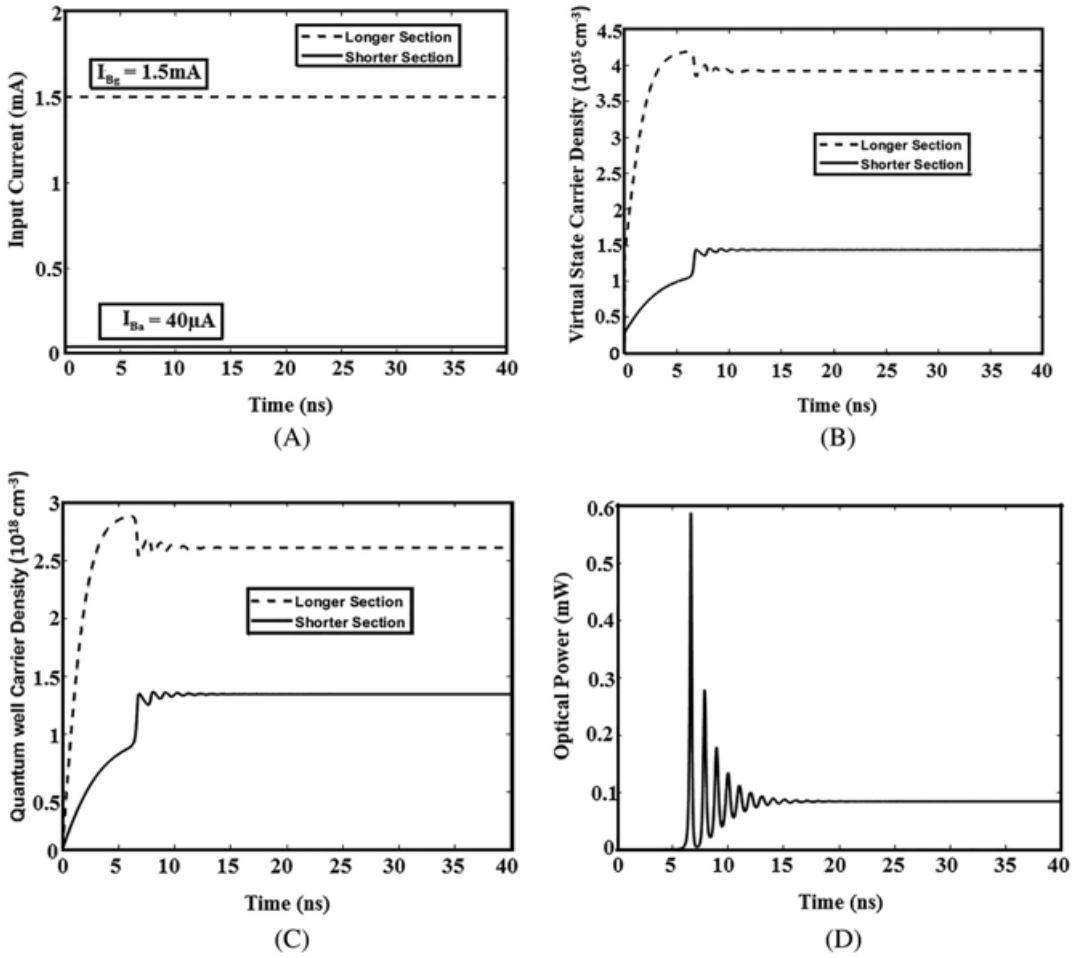

FIGURE 7 Transient analysis of dual base transistor laser (TL) after threshold: (A) input currents, (B) virtual state carrier density, (C) quantum well carrier density, and (D) optical power

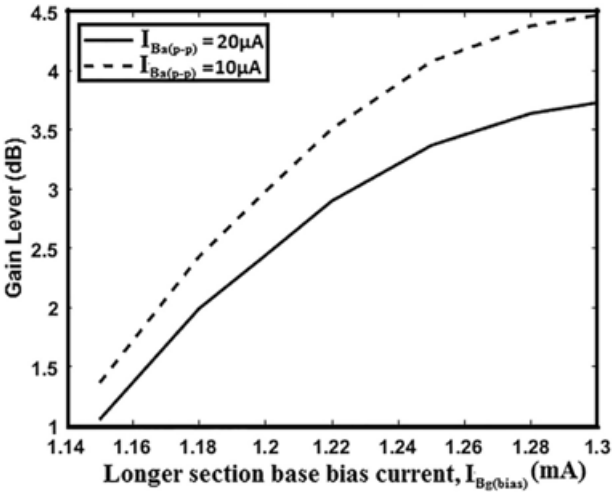

FIGURE 8 Gain lever (dB) of transistor laser (TL) under CE configuration

and the carrier concentrations in the longer section and shorter section are compliment to each other. From Figure 7, it is observed that the carrier density in both longer and shorter sections are capped to a value once the optical power reaches the threshold, thus the stimulated emission becomes dominant. Settling time, the time required to reach the steady state optical power decreases for increase in the input current.

3.3 | Analysis of gain lever effect

Gain lever is defined as the process of magnification of a optical gain achieved by laser devices due to nonlinear effects. Increasing the differential slope efficiency of optical power versus input current finds enormous applications in optical communication system, due to improved modulation characteristics. Increasing the differential slope efficiency increases the modulation depth or gain achieved in direct modulation systems. Gain lever in TL is evaluated by solving the following Equation (8).

$$\mathrm{GL_{dB}} = 10\log\frac{\eta_c\left(i_g, i_a\right)}{\eta_c^{\mathrm{normal}}} \tag{21}$$

where, the gain amplification in dual base TL is defined with respect to normal TL in decibels. $\eta_c\left(i_g, i_a\right)$ gives the differential slope of the dual base TL by varying the shorter section current with constant longer section bias current, derived from Figure 5A. η_c^{normal} is the differential slope of

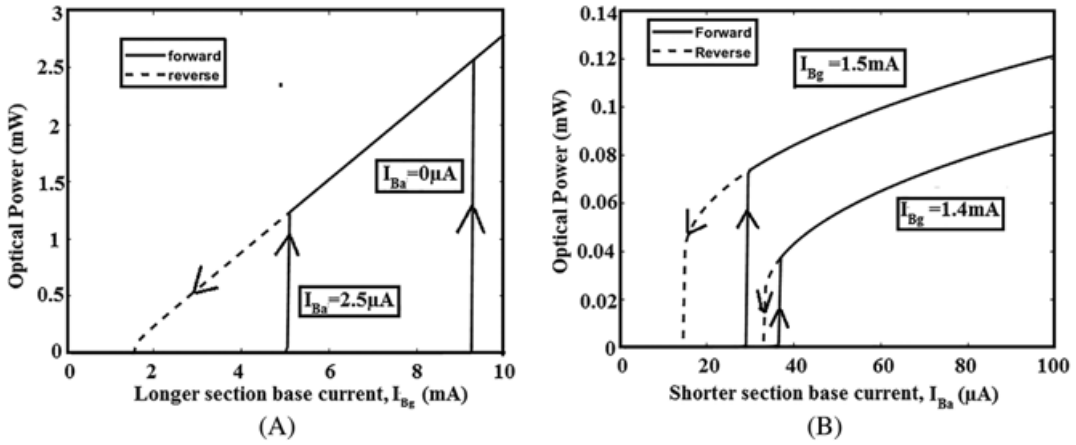

FIGURE 9 Optical power—current characteristics with (A) different shorter section (I_{Ba}) bias currents (B) different longer section (I_{Bg}) bias currents

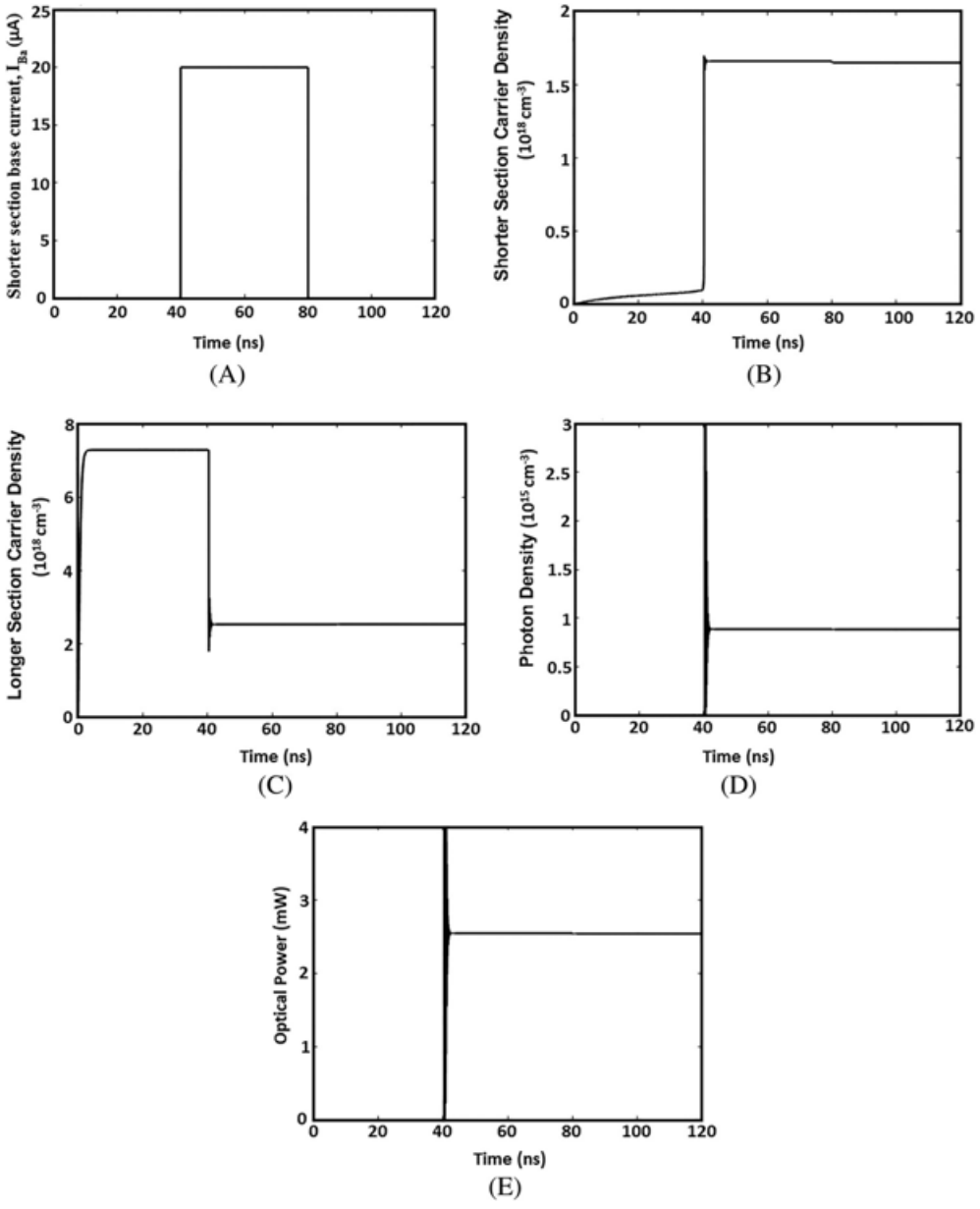

FIGURE 10 Pulse analysis: (A) input shorter section current pulse, (B) shorter section QW carrier density, (C) longer section QW carrier density, (D) photon density, and (E) optical power

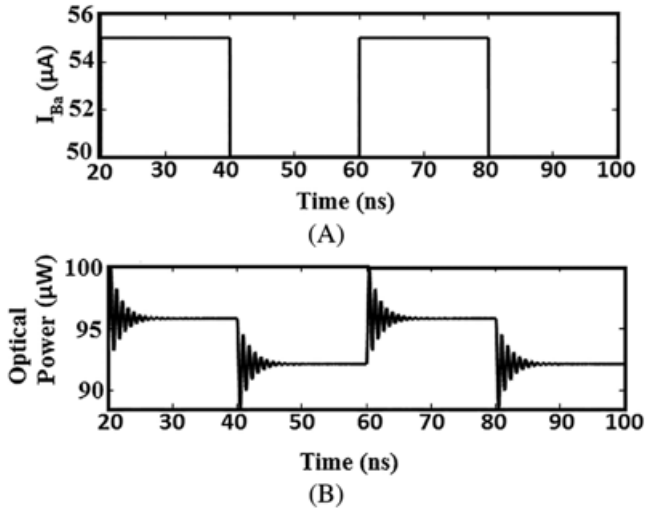

FIGURE 11 Dual base transistor laser: (A) input shorter section pulse current and (B) output optical pulse

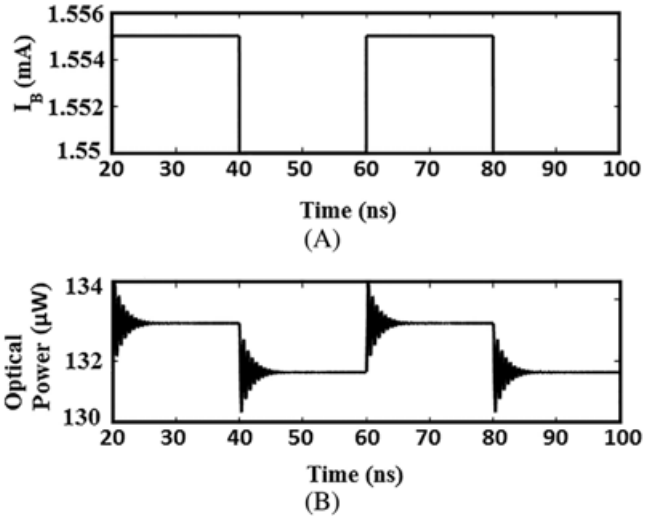

FIGURE 12 Normal transistor laser: (A) input pulse current and (B) output optical pulse

the normal TL obtained from Figure 3. Enhancement in gain or modulation efficiency is analyzed for TL under CE configuration for different longer section bias currents with shorter section bias currents are chosen near to the threshold.

From Figure 8 it is observed that the gain lever decreases for increase in peak-peak amplitude of RF current applied to the shorter section of the TL.

3.4 | Bisatbility

The bistable behavior in dual base TL is analyzed and plotted in Figure 9. Forward and reverse currents are applied for one section by fixing the other section current as constant. Optical power for different longer section current (I_{Bg}) in both forward and reverse directions with fixed shorter section bias currents ($I_{Ba[bias]}$) is plotted in Figure 9A. It is observed that the hysteresis width reduces for increase in the shorter section current. It is also found that the optical power values for switch off current are closer approximately to each other for different shorter section bias current ($I_{Ba[bias]}$). From Figure 9B, it is found that the hysteresis width increases for increasing the longer section bias current ($I_{Bg\ [bias]}$) for different shorter section current (I_{Ba}).

Bistability in a TL is further analyzed by providing an input electrical current pulse to the shorter section and biasing the longer section with constant DC current. Longer section DC bias current is chosen as 9.2 mA from Figure 9A (after threshold) with shorter section pulse varying from 0 to 20 μA as shown in Figure 10A.

It is found that after switching the input current pulse to 20 μA, the TL becomes ON and optical power switches to its maximum value as shown in Figure 10E. It is also found that longer section quantum well carrier density reaches minimum value, so longer section can have maximum photon generation.

After switching the input current pulse to 0 μA and keeping the longer section bias current as 9.2 mA, the optical power maintains the ON condition and so the dual base TL exhibits two states for same input current as shown in Figure 10E. Hence it observed that the TL exhibits the bistability behavior.

Transient analysis of bistability in dual base TL is analyzed by applying a pulse current as an input to the shorter section and dc bias current of $I_{Bg(bias)} = 1.5$ mA to the longer section as shown in Figure 11.

It is compared with normal TL by applying an input pulse current with amplitude being equal to the addition of longer and shorter section currents ($I_B = I_{Bg} + I_{Ba}$) for level 1 and 0 as shown in Figure 12. The ER of the generated optical pulse is compared between normal TL and dual base TL.

$$\mathrm{ER} = 10\log\frac{P_1}{P_0} \tag{22}$$

ER is defined as the ratio of optical power level corresponding to bit 1 to the optical power level corresponding to bit 0.[9] A high value of ER is expected to achieve a best link performance.

From Figures 11 and 12, it is observed that in dual base TL optical power level for bit 1 is $P_1 = 95.8$ μW and optical power level for bit 0 is $P_0 = 92.2$ μW and in case of normal TL is $P_1 = 133.2$ μW and $P_0 = 131.6$ μW. Based on the Equation (22) it is found that ER for dual base TL is 0.17 dB and for normal TL is 0.05 dB. It is observed that the ER of dual base TL is 0.12 dB higher than the normal TL.

4 | CONCLUSION

Gain lever and optical bistability effects in TL are analyzed by splitting the active region of the TL in to two sections with unequal length. DC characteristics of gain lever TL

under CE configuration is analyzed and compared with the normal TL. Varying the shorter section current with constant longer section current shows that the gain lever TL enters into a bistable switching state. A maximum of 4.5 dB enhancement in gain is observed under the bias current of 1.3 mA applied to the longer section of the TL. ER improvement of 0.12 dB compared with normal TL is observed with the bias current of 1.5 mA applied to the longer section of the TL.

CONFLICT OF INTEREST

The authors declare no conflicts of interest.

DATA AVAILABILITY STATEMENT

Research data are not shared.

REFERENCES

[1] Lasher GJ. Analysis of a proposed bistable injection laser. *Solid State Electron*. 1964;7:707-716.

[2] Ueno M, Lang R. Conditions for self-sustained pulsation and bistability in semiconductor lasers. *Appl Phys Lett*. 1985;58:1689.

[3] Vahala KJ, Newkirk MA, Chen TR. The optical gain lever: a novel gain mechanism in the direct modulation of quantum well semiconductor lasers. *Appl Phys Lett*. 1989;54:2506-2508.

[4] Moore N, Lau KY. Ultrahigh efficiency microwave signal transmission using tandem contact single quantum well GaAlAs lasers. *Appl Phys Lett*. 1989;55:936-938.

[5] Duan G-H, Landais P, Jacquet J. Modeling and measurement of bistable semiconductor lasers. *IEEE J Quantum Electron*. 1994; 30(11):2507-2515.

[6] Seltzer CP, Westbook LD, Wickes HJ. The "gain-lever" effect in InGaAsP/InP multiple quantum well lasers. *J Light Technol*. 1995;13(2):283-289.

[7] Wang J-Y, Cada M, Van Dommelen R, Makino T. Dynamic characteristics of bistable laser diodes. *IEEE J Sel Top Quantum Electron*. 1997;3(5):1271-1279. doi:10.1109/2944.658607

[8] Pocha MD, Goddard LL, Bond TC, et al. Electrical and optical gain lever effects in InGaAsDouble quantum-well diode lasers. *IEEE J Quantum Electron*. 2007;43(10):860-868.

[9] Piramasubramanian S, Ganesh Madhan M, Sindhuja A. Performance analysis of a digital fiber optic link incorporating gain-levered laser diode transmitter. *Int J Numer Model*. 2018;31:e2321.

[10] Piramasubramanian S, Madhan MG. Simultaneous reduction of IMD3 and IMD5 in bisection laser diode by feedback second harmonic injection. *Opt Commun*. 2014;328:151-160.

[11] Keiser G. *Optical Fiber Communication*. McGraw Hill Education; 2017.

[12] Al-Rawesshidy H, Komaki S. *Radio over Fiber Technologies for Mobile Communications Networks*. Artech House; 2002.

[13] Coldren LA, Corzine SW, Masanovic ML. *Diode Lasers and Photonic Integrated Circuits*. 2nd ed. John Wiley & Sons; 2012.

[14] Walter G, Holonyak N Jr, Feng M, Chan R. Laser operation of a heterojunction bipolar light-emitting transistor. *Appl Phys Lett*. 2004;85:4768-4770.

[15] Feng M, Holonyak N Jr, Walter G, Chan R. Room temperature continuous wave operation of a heterojunction bipolar transistor laser. *Appl Phys Lett*. 2005;87:131103.

[16] Then HW, Walter G, Feng M, Holonyak N Jr. Charge control analysis of transistor laser operation. *Appl Phys Lett*. 2007;91: 243508.

[17] Sato N, Shirao M, Sato T, et al. Design and characterization of AlGaInAs/InP buried heterostructure transistor lasers emitting at 1.3μm wavelength. *IEEE J Sel Top Quantum Electron*. 2013;19 (4):1502608-1502608.

[18] Zhang L, Leburton J-P. Modeling of the transient characteristics of heterojunction bipolar transistor lasers. *IEEE J Quantum Electron*. 2009;45:359-366.

[19] Faraji B, Shi W, Pulfrey DL, Chrostowski L. Analytical modeling of the transistor laser. *IEEE J Sel Top Quantum Electron*. 2009; 15(3):594-603.

[20] Shirao M, Lee SH, Nishiyama N, Arai S. Large signal analysis of a transistor laser. *IEEE J Quantum Electron*. 2011;47(3):359-367.

[21] Ranjith R, Piramasubramanian S, Ganesh MM. Distortion analysis of 1.3μm AlGaInAs/InP transistor laser. In: Bhattacharya I, Chakrabarti S, Reehal H, Lakshminarayanan V, eds. *Advances in Optical Science and Engineering. Springer Proceedings in Physics*. Vol 194. Springer; 2017.

[22] Ranjith R, Piramasubramanian S, Ganesh Madhan M. Effect of number of quantum wells on modulation and distortion characteristics of transistor laser. *Opt Laser Technol*. 2022;147:107655. doi:10.1016/j.optlastec.2021.107655

[23] Vinodhini SV, Piramasubramanian S, Ganesh Madhan M. Analysis of nonlinear distortion and its reduction using feedback injection schemes in an 1.3 μm transistor laser, 439. *Opt Commun*. 2019;439:224-232.

How to cite this article: Ranjith R, Piramasubramanian S, Ganesh Madhan M. Numerical simulation and analysis of dual base transistor laser. *Microw Opt Technol Lett*. 2022;64:962–971. doi:10.1002/mop.33186